molecular pharmaceutics

pubs.acs.org/molecularpharmaceutics

Communication

Restoring Endogenous Repair Mechanisms to Heal Chronic Wounds with a Multifunctional Wound Dressing

Rahimeh B. Atashgah, Amir Ghasemi, Mohammad Raoufi,* Mohammad-Amin Abdollahifar, Steven Zanganeh, Hossein Nejadnik, Alieh Abdollahi, Shahriar Sharifi, Baltazar Lea, Miguel Cuerva, Mehdi Akbarzadeh, Carmen Alvarez-Lorenzo, Seyed Nasser Ostad, Andrea S. Theus, Doris L. LaRock, Christopher N. LaRock, Vahid Serpooshan, Rouzbeh Sarrafi, Ki-Bum Lee, Hojatollah Vali, Holger Schönherr, Lisa Gould, Pablo Taboada, and Morteza Mahmoudi*

Cite This: *Mol. Pharmaceutics* 2021, 18, 3171−3180

Read Online

ACCESS | Metrics & More | Article Recommendations | Supporting Information

ABSTRACT: Current treatment of chronic wounds has been critically limited by various factors, including bacterial infection, biofilm formation, impaired angiogenesis, and prolonged inflammation. Addressing these challenges, we developed a multifunctional wound dressing-based three-pronged approach for accelerating wound healing. The multifunctional wound dressing, composed of nanofibers, functional nanoparticles, natural biopolymers, and selected protein and peptide, can target multiple endogenous repair mechanisms and represents a promising alternative to current wound healing products.

KEYWORDS: *chronic wounds, multifunctional wound dressing, nanomedicine, endogenous repair*

Although chronic wounds have different types, they generally exhibit failure to recover anatomic and functional integrity due to infection, unresolved inflammation, and severe impairment of healing processes, including angiogenesis, epithelial migration, and cell proliferation.[1−4] The central challenge of the current solutions in healing chronic wounds is that majority of them addresses one of the predetermined issues of the complex wound environment.[4] Therefore, the development of a multifunctional patch that addresses some of these issues at the same time is of a significant clinical interest. To achieve a multidisciplinary view on the wound healing ecosystem and identify unmet clinical needs, we interviewed over 100 wound healing experts (e.g., clinicians, dressing developers, and directors of wound healing centers) through the I-Corps program funded by the National Science Foundation.[5]

Clinical success in curing chronic wounds is limited in large part due to a lack of understanding of the mechanical, biochemical, immunological, and repair processes involved in skin regeneration as well as their interplay.[6−11] Numerous types of wound dressings have been proposed and developed to treat chronic wounds and promote healing, with some having positive effects. However, the limitations of the more successful wound dressings, such as weak adhesiveness and inadequate mechanical properties, e.g., low flexibility, extensibility, and elasticity, require the application of secondary dressings, which in turn increases the risk of infection.[12−14] Notably, most of these dressings are designed to restore only one of the many impaired healing processes and hence achieve only limited success.[9,15−18] The use of natural tissues (e.g., human cadaver skin, placental membrane, porcine intestinal submucosa, and neonatal foreskin) can address the aforementioned issues in healing chronic wounds. However, owing to the requirement for decellularization, natural tissue harvesting is a prolonged and expensive process incapable of further cost reduction due to the scarcity of ingredients and the in-depth testing of donor skin followed by chemical processing and storage. Furthermore, tissue-based products comprising live cells have strict shipping and application requirements. The temperature of the product has to be carefully controlled in transit (dry ice), and the patient must receive the graft within hours after the product arrives at wound centers. Furthermore, stringent wound bed preparation requirements make them inappropriate in all but the hospital setting. There is, therefore, a large and growing need for the development of effective chronic wound treatments that is affordable, efficient, and easy to use.[19]

In this paper, we report on the development of an easy next-generation "composite patch" dressing for chronic wounds that (1) provides an environment with suitable physicomechanical properties, (2) delivers superparamagnetic iron oxide nanoparticles (SPIONs) to minimize and counteract microbial biofilm formation, which can otherwise lead to infection and prolonged inflammation, (3) delivers follistatin like-1 (FSTL-1) proteins that accelerate healing by the induction of angiogenesis and cell proliferation and reducing the chance of overgrowth of skin cells, and (4) releases pro-resolving

Received: May 17, 2021
Revised: July 7, 2021
Accepted: July 9, 2021
Published: July 19, 2021

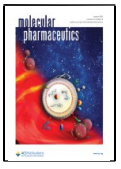

https://doi.org/10.1021/acs.molpharmaceut.1c00400
Mol. Pharmaceutics 2021, 18, 3171−3180

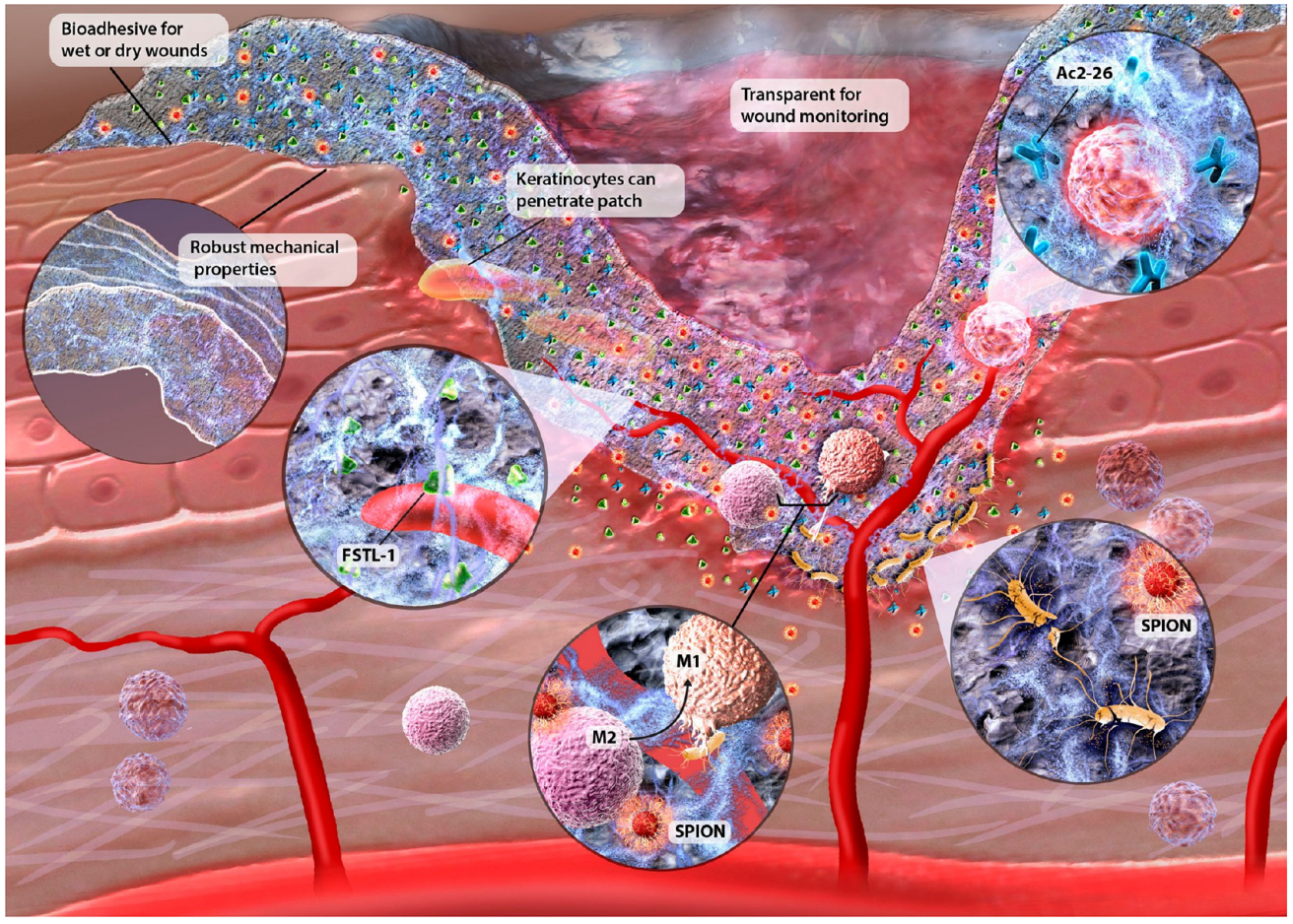

Figure 1. Mechanism of orchestrated action of the next-generation composite patch dressing for healing chronic wounds. The patch contains nanofibers composed of collagen, chondroitin sulfate, hyaluronic acid, elastin, and chitosan to closely mimic the flexibility, stiffness, and adhesiveness of human skin. The nanofibrils also contain FSTL-1 protein and AC2-26 peptides. The sustained release of FSTL-1 promotes angiogenesis as well as keratinocyte migration and proliferation. SPIONs, which are physically attached to the patch surface, induce macrophages to shift from a M2 to a M1 phenotype, and promote biofilm removal by phagocytosis. As the patch degrades, Ac2-26 will be released to help terminate prolonged inflammation, promote fibroblast migration, and reduce scarring.

inflammatory mediators (i.e., AC2-26) to tamp down the unbalanced inflammation of the wound site[20−23] (see Figure 1 for details).

Bacterial infections associated with biofilm formation can reduce the efficacy of the host response and considerably delay wound healing. Chitosan in our patch is well-known for its bacteriostatic properties due to interactions between charged groups in the chitosan backbone and bacterial wall constituents.[24] To further enhance the antimicrobial activity, our patches were laden with ferumoxytol (as FDA-approved SPIONs). Our studies show these SPIONs possess two unique functions: (1) an intrinsic antibacterial activity[25,26] and (2) the ability to shift macrophage polarization from M2 to M1.[27,28] Macrophages in chronic wounds exhibit reduced capacity to phagocytose dead neutrophils and reduced apoptotic clearance.[29−31] Shifting the polarization to M1 can help to restore the desired macrophage capacity.

Chronic wounds are typically characterized by inadequate angiogenesis and impaired extracellular matrix (ECM) production. We recently found that FSTL-1 induces proliferation of adult cardiomyocytes following myocardial infarction to help regenerate cardiac tissue.[32] FSTL-1 also promotes keratinocyte migration during re-epithelization in healing skin.[33] FSTL-1 is very low/undetectable in healthy unwounded skin but is abundant in wounded skin, reflecting its critical role in wound healing. Remarkably, FSTL-1 is not expressed in chronic nonhealing ulcer wounds in diabetics.[34,35] Another reason to incorporate FSTL-1 into our patch is that FSTL-1 can bind activin proteins to antagonize their adverse effects (e.g., skin tumorigenesis and scar formation) during wound healing.[36−40] We homogeneously incorporate FSTL-1 into the patch using nanoextrusion so there can be sustained release of FSTL-1, during the patch degradation process, into the wound bed to induce angiogenesis, promote keratinocyte migration and proliferation, and increase healing.

Table 1. Composition of the Nanofibrous Patch

protein/polymer	buffer[a]	concentration (mg/mL)	portion (%)
chitosan	acetic acid (1%)/PBS	3.5	80
collagen	PBS	0.3	5
chondroitin sulfate	PBS	0.5	5
elastin	PBS	0.3	5
hyaluronic acid	PBS	0.5	5

[a]PBS: phosphate buffered saline

https://doi.org/10.1021/acs.molpharmaceut.1c00400
Mol. Pharmaceutics 2021, 18, 3171−3180

Table 2. Composition and Properties of the Designed Patch Systems

patch	composition	remarks
nanofibrous patch	Extruded nanofibrous patch composed of chitosan, collagen, chondroitin sulfate, elastin, and hyaluronic acid	Providing a suitable environment in which cells can easily proliferate, rapidly multiply, and form new blood vessels
FSTL-1 patch	Extruded nanofibrous patch composed of chitosan, collagen, chondroitin sulfate, elastin, hyaluronic acid, and follistatin like-1	Providing a suitable environment in which cells can easily proliferate, rapidly multiply, and form new blood vessels; accelerating angiogenesis process
AC2-Z6 patch	Extruded nanofibrous patch composed of chitosan, collagen, chondroitin sulfate, elastin, hyaluronic acid, and pro-resolving AC2-26 peptide	Providing a suitable environment in which cells can easily proliferate, rapidly multiply and form new blood vessels; minimizing unbalanced and prolonged inflammation
SPION patch	Incubated superparamagnetic iron oxide nanoparticles with the extruded nanofibrous patch composed of chitosan, collagen, chondroitin sulfate, elastin, and hyaluronic acid	Providing a suitable environment in which cells can easily proliferate, rapidly multiply and form new blood vessels; preventing and reducing existing bacterial infection
composite patch	Incubated superparamagnetic iron oxide nanoparticles with the extruded nanofibrous patch composed of chitosan, collagen, chondroitin sulfate, elastin, hyaluronic acid, follistatin like-1, and pro-resolving AC2-26 peptide	Providing a suitable environment in which cells can easily proliferate, rapidly multiply and form new blood vessels; preventing and reducing existing bacterial infection; minimizing unbalanced and prolonged inflammation; and accelerating angiogenesis process

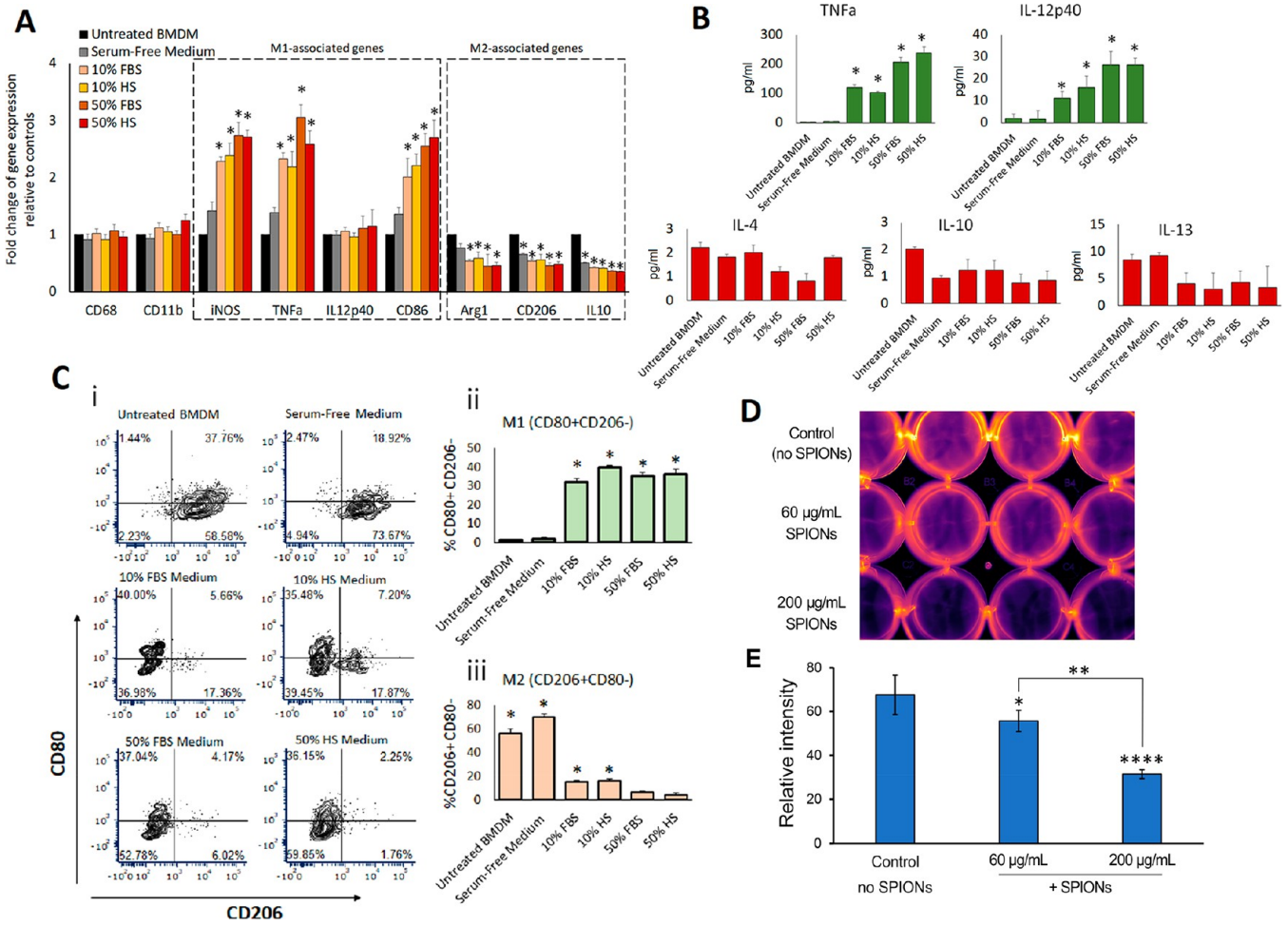

Figure 2. SPIONs activate macrophages and in the presence of macrophages reduce *S. aureus* biofilms drastically. (A) Treatment of bone marrow-derived macrophages with bare and corona coated ferumoxytol (with various concentrations of human and fetal bovine serum) shows upregulation of proinflammatory genes (INOS, Il-12p40, and CD86) and a downregulation of anti-inflammatory genes (Arg1, Il-10, and CD206) over 24 h, as measured by quantitative RT-PCR. (B) Indicated cytokines in BMDM/ferumoxytol mixed supernatants as assessed by Luminex multiplex cytokine analysis (right). (C) (i) Representative flow cytometry assay for bone marrow-derived macrophages polarization treated with ferumoxytol in different human and fetal bovine serum concentrations. (ii) CD80+CD206− (M1 macrophages) were significantly increased in the presence of 10% and 50% FBS and human sera in the culture media. (iii) CD206+CD80− (M2 macrophages) were significantly decreased in serum-free culture media. (D−E) GFP: labeled *S. aureus* were cocultured with human THP-1 macrophages for 24 h in 24-well tissue culture plates, using DMEM containing 0, 60, and 200 μg/mL of pristine SPIONs. Heat map images showing relative GFP signal intensities after the 24 h culture and (D) were quantified using ImageJ (E).

Besides FSTL1, we added Ac2-26, a peptide derived from the *N*-terminus of annexin A1 (ANAX1),[41−44] as a stable pro-resolving inflammatory mediator. Ac2-26 replicates the anti-inflammatory maintenance of cytoskeleton and ECM, tissue growth, apoptosis, and differentiation effects of ANAX1.[45] Topically controlled release or encapsulated formulation of Ac2-26 can stimulate fibroblast migration in vitro and in

https://doi.org/10.1021/acs.molpharmaceut.1c00400
Mol. Pharmaceutics 2021, 18, 3171−3180

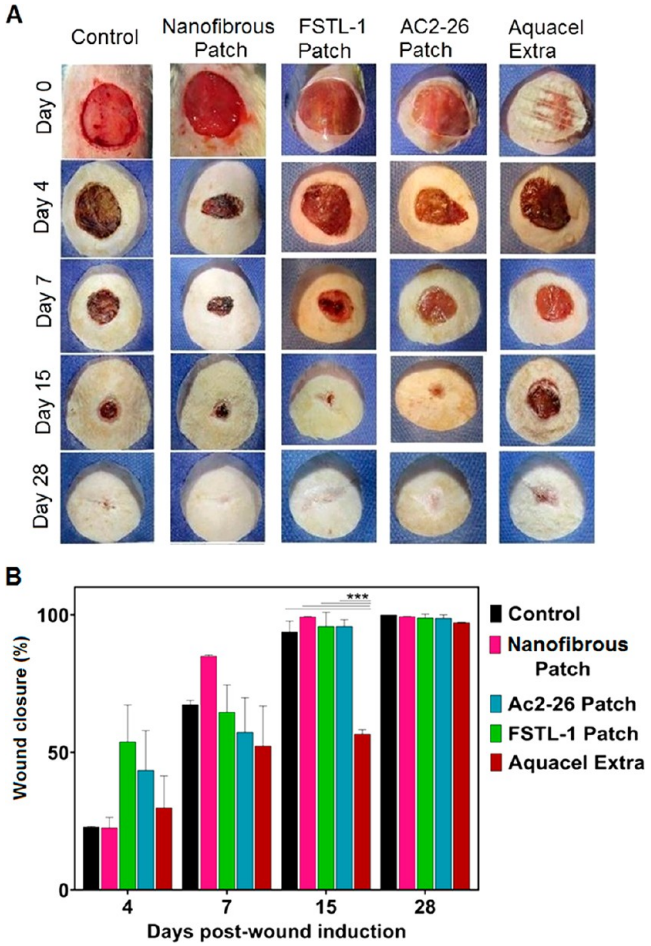

Figure 3. Images of wound contraction after intervention in *noninfected* diabetic rat model 4, 7, 15, and 28 days after wound induction. (A) A diabetic wound in a rat model at determined time points, wound induction day, 4, 7, 15, and 28 days treated with AQUACEL Extra, nanofibrous patch, FSTL-1 patch, AC2-26, and control group (B) Wound closure % (size of closure/entire size of each wound) of uninfected diabetic rats.

vivo.[45,46] Ac2-26 significantly improves wound healing in animal models even in the presence of high glucose.[45,46]

RESULTS AND DISCUSSION

To provide an environment with suitable physicomechanical properties, we used a dedicated template-assisted nanoextrusion technique (exploiting nanoporous anodic aluminum oxide, AAO, membranes) and thereby fabricated a multifunctional nanofibrous composite patch composed of a careful selection of natural biopolymers consisting of collagen, elastin, chitosan, chondroitin sulfate, and hyaluronic acid (Table 1). The selection of biopolymers was based on (i) minimizing and counteract microbial biofilm formation with chitosan that has proven antibacterial capability,[47−51] which can otherwise lead to infection and prolonged inflammation, (ii) accelerating healing by the induction of angiogenesis through the use of collagen type I,[52−55] and (iii) tamp down the unbalanced inflammation of the wound site using synergist roles of chondroitin sulfate and hyaluronic acid.[52−58] We have thoroughly evaluated the physicochemical and mechanical properties of the resulting patches using techniques including Fourier transform infrared (FTIR) spectroscopy, differential scanning calorimetry (DSC), thermogravimetric analysis (TGA), Brunauer−Emmett−Teller (BET), and scanning electron microscopy (SEM) (Figures S1−S8 in the Supporting Information (SI)). Through this vast combination of characterization approaches, we found and confirmed that the patches possess the capacity to (1) mimic the flexibility, stiffness, and adhesiveness of human skin, (2) provide a suitable environment for tissue regeneration, and (3) uniformly distribute a mixture of biopolymers and therapeutic biomolecules (although it needs further research to evaluate the degree of uniformity), including FSTL-1 and AC2-26, to accelerate wound healing (see Table 2 for all of the employed wound healing patches in this study).

We validated the hypothesis that macrophage activation by ferumoxytol may contribute to antibacterial activity in the wound and reduce bacterial infection by modulating macrophage polarization (Figure 2).

As some of the chronic wounds have exudates,[19] which are fluids with various types of proteins, cytokines, and other types of biomolecules, they may interact with the surface of nanoparticles and create protein corona[19,59,60] (i.e., a layer of biomolecules that covers the surface of nanoparticles and affect their interactions with biosystems[61−63]). As a proof-of-concept study, we considered the role of protein corona formation in macrophage polarization. Our systematic investigations revealed that ferumoxytol significantly upregulates TNF-α, iNOS, and CD86 markers, indicating polarization of macrophages to the proinflammatory phenotype (M1) but only in corona coated nanoparticles (Figure 2A). By contrast, the mRNA levels of anti-inflammatory CD206, ARG1, and IL10 markers were observed to be significantly reduced after exposure to SPIONs without a protein corona. Similarly, the production of proinflammatory cytokines, such as TNF-α and Il-12p40, significantly increased in the serum-containing media, but no significant production of anti-inflammatory cytokines, such as IL-10, IL4, and IL13, was observed (Figure 2B). The enhanced production of TNF-α has a beneficial effect on the wound-healing process, as it can induce the expression of vascular endothelial growth factor A in keratinocytes and fibroblasts.[64,65] It is noteworthy that the roles of activation and tempering the inflammation are designed to be sequential: first, proinflammatory effects of SPIONs help preventing bacterial infections, and then the anti-inflammatory effects of AC2-26 reduce the prolonged inflammation. TNF-α can also enhance the synthesis of a wide range of metalloproteinases (MMPs), including MMP-1, MMP-2, MMP-3, MMP-9, MMP-13, and MT1-MMP.[65−69] MMPs possess a crucial role in several stages of the wound-healing process by facilitating cell migration and tissue remodeling.[70,71]

The phenotypic heterogeneity of macrophages was also measured by flow cytometry, using a combination of CD80 and CD206 lineage markers. All macrophages interacting with SPIONs in serum-containing media exhibited a significant increase in CD80+CD206− (M1) expression and a significant decrease in CD206+CD80− (M2) expression in comparison with control and serum-free conditions (Figure 2C). These results indicate that the absence of serum proteins in the media constitutively limits the SPIONs-dependent function of macrophages. In other words, the interaction of the SPIONs with wound exudate and drainage fluid can further promote macrophage M1 activation, which supports bacterial removal.

To confirm the antibacterial role of the SPIONs, GFP-labeled *S. aureus* were 2D cultured in concentrations of 0, 60,

https://doi.org/10.1021/acs.molpharmaceut.1c00400
Mol. Pharmaceutics 2021, 18, 3171−3180

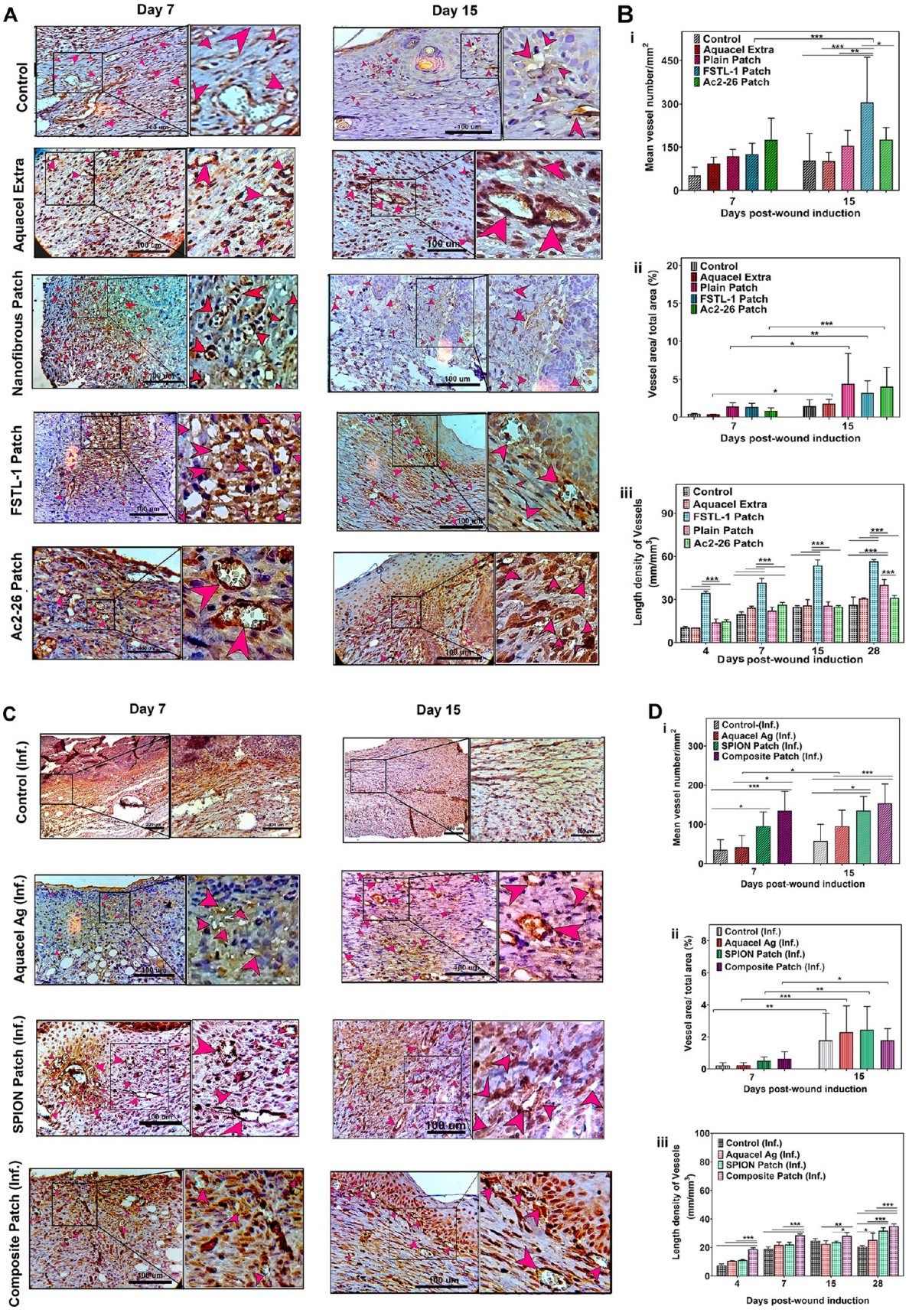

Figure 4. Immunohistochemical analysis of angiogenesis at the wound site. (A) Representative images of vWF staining in noninfected diabetic groups: Control, nanofibrous patch, AQUACEL Extra, FSTL-1 patch, and Ac2-26 patch at (i, iii, v, vii, ix) 7 and (ii, iv, vi, viii, x) 15 days postwound induction, respectively. Scale bars: 100 μm. (B) Quantitative analysis of angiogenesis and maturation of capillary vessels 7 and 15 days after wound induction: (i) numerical density of capillary vessels, (ii) total area of vessels, (iii) stereological analysis of length density of blood vessels at the

https://doi.org/10.1021/acs.molpharmaceut.1c00400
Mol. Pharmaceutics 2021, 18, 3171−3180

Figure 4. continued

wound site. (C) Representative images of vWF staining in infected diabetic groups: Control (inf), AQUACEL Ag, FSTL-1 patch, and Ac2-26 patch at (i, iii, v, vii) 7 and (ii, iv, vi, viii) 15 days postwound induction, respectively. Scale bars, 100 μm. (D) Quantitative analysis of angiogenesis and maturation of capillary vessels 7 and 15 days after wound induction: (i) numerical density of capillary vessels, (ii) total area of vessels, (iii) stereological analysis of the length density of blood vessels at wound site showing the effective role of FSTL-1 on angiogenesis and vessel development. The results are mean ± SD, * $p < 0.05$, ** $p < 0.01$, *** $p < 0.001$. The microvessels with 10−15 μm diameter are considered capillary vessels (a surface area about 100 μm^2).

and 200 μg/mL of SPIONs in DMEM for 24 h in the presence of human monocyte-derived macrophages (THP-1; Figure 2D,E). On the basis of the GFP signal analysis, a significant reduction in *S. aureus* was observed when they were cultured with 60 and 200 μg/mL of SPIONs, in comparison to the control group (no SPIONs) ($P < 0.05$ and 0.0001, respectively) (Figure 2E). Increasing SPION concentrations from 60 to 200 μg/mL resulted in a further increase in bacteriostatic activity ($P = 0.0008$).

We carefully analyzed the effect of each component (i.e., SPIONs, FSTL-1, or AC2−26) added to the patch (i.e., an extruded nanofibrous patch composed of chitosan, collagen, chondroitin sulfate, elastin, and hyaluronic acid) and probed the resulting antibacterial properties, angiogenesis induction, and pro-resolving inflammation properties in vivo using a diabetic wound rat model. The study revealed the prominent role of SPIONs, FSTL-1, and AC2−26 in removing bacterial infection, inducing the formation of new vessels and reducing the inflammation intensity, respectively, in the healed wound sites (Figures S9−S18 in SI).

We also probed the therapeutic efficacy of composite patches (i.e., nanofibrous patches containing SPIONs, FSTL-1, and AC2-26) on both clean and bacteria inoculated wounds. The wounds inoculated with *S. aureus* (5×10^6 CFU/μL).

The data revealed a significantly enhanced healing efficacy of the composite patch compared to other patches. Figure 3A represents wound closure during one-month postintervention using the designed nanofibrous patches, FSTL-1 patches, and AC2-26 patches on noninfected diabetic rats in comparison with AQUACEL Extra and control group (without any intervention after wound excision). Digital planimetry of noninfected diabetic wounds showed significant wound closure after 4 weeks with all treatments. Wound closures with nanofibrous patches, FSTL-1 patches, Ac2-26 patches, AQUACEL Extra treated groups, and the control group 4 days postwound induction were 23 ± 4%, 54 ± 13%, 43 ± 14%, and 30 ± 12%, respectively. Wound closures at 1 week after wounding demonstrated faster healing rates with the Ac2-26, FSTL-1, and nanofibrous patches compared with AQUACEL Extra and the control group (57 ± 12%, 65 ± 10%, 85 ± 1%, 52 ± 14%, 67 ± 2%, and 23 ± 1%, respectively). Wound closure of AQUACEL Extra after 2 weeks of wound induction was significantly lower than other groups, including the control group (57 ± 2%, $P < 0.001$). Complete wound closure in all experimental groups was observed after four weeks, and there was no significant difference among groups after 28 days of wound excision Figure 3B.

We found that FSTL-1 patches induced capillary formation at the wound site significantly better than the other patches. FSTL-1 induces neovascularization and blood vessel maturation in vivo. Von Willebrand Factor (vWF) staining revealed regenerated tissue with more blood vessels in the groups contain FSTL-1 (Figure 4A) and composite patches (Figure 4C) compared with the other groups (Figure 4A). The quantified density of newly formed capillary vessels two weeks after applying the FSTL-1 patch (305 ± 156) was significantly higher than for the Ac2-26 patches (176 ± 42, $p < 0.05$), the nanofibrous patches (154 ± 55, $P < 0.01$), and the control (103 ± 94, $P < 0.01$) groups (Figure 4Bi). Statistical analysis of total vessel area between the groups showed enhanced blood vessel formation in patch-treated wounds (Figure 4Bii). In addition, stereology assessment of new capillary vessel length and density (Figure 4Biii) showed that capillary vessel formation was much greater with FSTL-1 and composite patches than with other patches. Overall, the composite patch exhibited all benefits of each patch (e.g., angiogenesis, antibacterial, and pro-resolving inflammation of FSTL-1, SPIONs, and AC2-26 patches respectively) simultaneously.

While these in vitro and animal study tests discussed above are necessary and relevant tests, human trials are required to assess the actual efficacy of the novel wound dressing. The therapeutic wound healing capability of the nanofibrous and composite patches was thus examined following the application to 13 patients (Figure 5) with nonhealing chronic diabetic wounds. These wounds had not previously healed despite the application of state of the art standard-of-care therapy (i.e., appropriate debridement, treatment of infection, and application of conventional moist dressings), and other available approaches (i.e., the use of commercial wound-healing products, including AQUACEL and GranuGel) (Figure 5A). Informed consent was obtained from all participants in this study. All required interventions during the study were carried out by experienced medical staff. In addition, the blood glucose levels were controlled. Patients treated with the nanofibrous patch showed a relatively fast average healing rate of 26 ± 18%/day. Variations in healing among the patients were likely related to their health conditions and the individual wound shape and dimensions. However, the chronic wounds of all 13 enrolled patients healed after treatment with the patches (Figure 5A). The wound size and complication of the patients' disease also affected the healing rate and follow-up period for each case. Overall, each case was followed up for at least two months.

In another case study, a 71-year-old male with an infected diabetic wound at the ankle (fibula) was treated with a novel composite patch (Figure 5D). The wound surface area was measured with digital planimetry (ImageJ software, 1.48 (v). Figure 5E shows the 14-week-old nonhealing chronic diabetic wound on the plantar fascia of this patient. Within 8 weeks after implantation of the nanofibrous patch, the wound was observed to be closed. It is noteworthy that each row demonstrates different wounds.

In summary, we have developed a multifunctional nanofibrous patch with a unique capacity to promote the body's endogenous capacity to heal chronic wounds. Our method relies on a composite patch that has the following vital features, including (i) providing a suitable environment, in which cells

https://doi.org/10.1021/acs.molpharmaceut.1c00400
Mol. Pharmaceutics 2021, 18, 3171−3180

A

Patient Age/ Sex	Diabetic/ non-diabetic	Wound stage	Ulcer duration	Ulcer area (Cm^2)	Healing rate (H.R) (% /day)	Depth (Cm)	Rate of healing wound volume /time (days)	Localization of ulcer	Duration of healing	Following time after healing (week)	Previous treatment
M-71	Diabetic	I	14 weeks	12.1	28.5	0.1	0.02	Plantar fascia	8 weeks	6	GranuGel
M-49	Diabetic	I	12 weeks	2.7	28.5	0.8	0.15	Foot	2 weeks	-	-
F-47	Diabetic	-	20 weeks	13.0	24	0.2	0.09	Forearm	4 weeks	4	-
F-76	Diabetic	-	15 weeks	11.0	11.9	0.1	0.01	Noise	12 weeks	8	Aquacel
F-47	Diabetic	I	16 weeks	12.5	16	0.2	0.09	Leg (Sura)	4 weeks	2	Agicoat
F-56	Diabetic	I	15 weeks	3.8	15.6	1.3	0.12	Foot	6 weeks	4	-
M-63	Diabetic/ Injured	I	21 weeks	14.9	47.6	0.1	0.07	Phalanges	20 days	-	-
M-28	Diabetic	-	3 weeks	5.7	47	-	-	forehead	3 weeks	4	-
M-69	Diabetic	I	20 weeks	47.0	12	0.1	0.06	Lower leg	11 weeks	8	GranuGel
M-53	Diabetic	I	2 weeks	7.5	71	0.5-1	0.40	Plantar fascia	2 weeks	3	GranuGel
F-56	Diabetic	I	2 weeks	76.5	17.4	1-1.5	1.71	Plantar fascia	8 weeks	8	Comfeel
M-63 *	Diabetic	I	2 weeks	2.7	17.8	0.5	0.02	First toe	8 weeks	4	-
				3.1	15.8	0.2	0.01	First toe	9 weeks	4	-
				10.6	15.8	0.4-0.7	0.1	Plantar fascia	9 weeks	4	-
M-71*	Diabetic	I	3 weeks	1.6	33.3	0.3	0.02	Ankle (fibula)	3 weeks	4	-

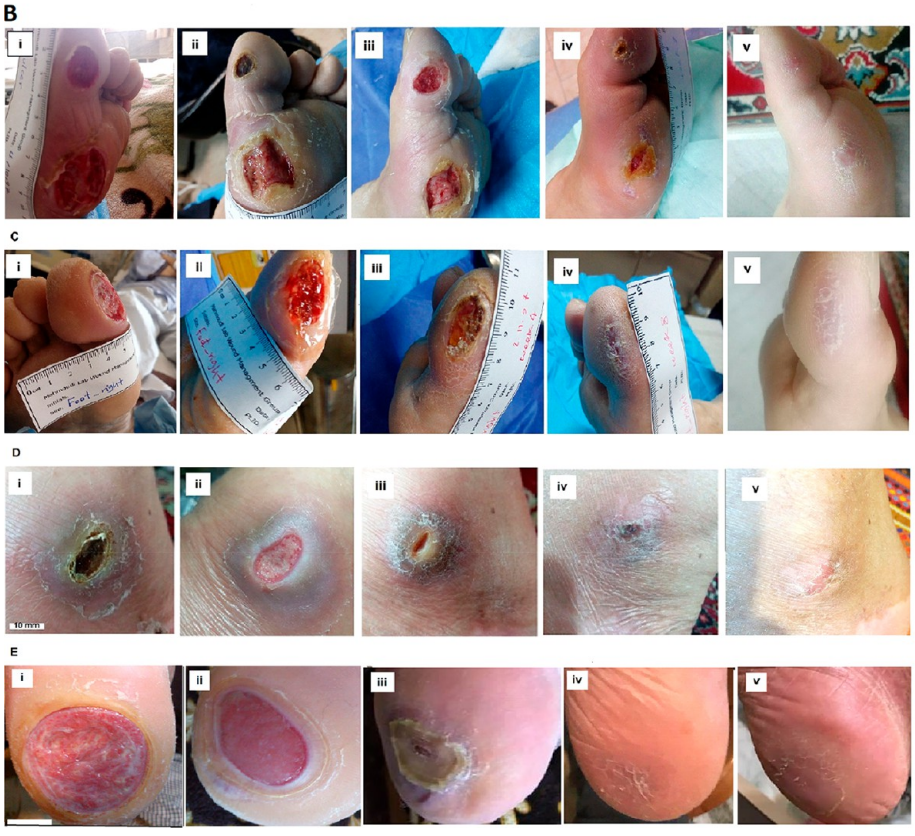

Figure 5. Results of the clinical study, in which patients were treated with the nanofibrous patch. (A) Table showing the characteristics of all participants (n = 13); ulcer duration indicates the time that the patients suffered from nonhealing chronic wounds that failed to heal on their own or with the use of available commercial products; the ulcer size was determined at the time the nanofibrous or composite (*) patch was applied. (B,C) A 63-year-old male with diabetic wounds (i) before and after (ii) 2, (iii) 4, (iv) 8 weeks, and (v) 12 weeks of treatment with the composite patch. (D) A 71-year-old male with a diabetic wound on the ankle (fibula) (i) before and after (ii) 7, (ii) 14, (iii) 18, (iv) 21 days, and (v) 7 weeks of treatment with composite patch. Scale bar, 1 cm. (E) An example of the wound healing capacity of the nanofibrous patch in a 71-year-old male with chronic diabetic wounds (i) before and after (ii) 3, (iii) 5, (iv) 7 weeks, and (v) 11 weeks of treatment initiation; Scale bar, 2 cm. The healing rate of the wound was calculated by the following equation: $\mathrm{HR\%} = 100\left[\frac{\frac{\pi}{4}(Ai - Af)}{\left((\mathrm{day}f - \mathrm{day}i)\frac{\pi}{4}Ai\right)}\right]$.

can easily proliferate and form new blood vessels (using FSTL-1), (ii) preventing or reducing existing bacterial infection using SPIONs with and without protein corona, and (iii) minimizing unbalanced and prolonged inflammation (using the Ac2-26

https://doi.org/10.1021/acs.molpharmaceut.1c00400
Mol. Pharmaceutics 2021, 18, 3171−3180

pro-resolving inflammatory mediator). This study could ultimately lead to the development of novel and efficient therapeutic wound healing patches that restore the body's natural healing process by reducing biofilm infections and adjusting the impaired angiogenesis and inflammation at the wound site. As recent reports revealed the critical role of sex in the safety and therapeutic efficacy of nanostructured materials,[72−74] further evaluations on the role of sex on the safety and efficacy of wound dressing consisting of nanomaterials are essential. Overall, the patch will substantially increase the likelihood of clinically relevant wound healing and minimize the risk of amputation in patients with chronic wounds.

■ ASSOCIATED CONTENT

Supporting Information

The Supporting Information is available free of charge at https://pubs.acs.org/doi/10.1021/acs.molpharmaceut.1c00400.

Full characterization of the multifunctional patch together with the complementary in vitro and in vivo outcomes (PDF)

■ AUTHOR INFORMATION

Corresponding Authors

Morteza Mahmoudi − *Precision Health Program, Michigan State University, East Lansing, Michigan 48824, United States; Department of Anesthesiology, Brigham & Women's Hospital and Mary Horrigan Connors Center for Women's Health & Gender Biology, Brigham & Women's Hospital, Harvard Medical School, Boston, Massachusetts 02115, United States;* orcid.org/0000-0002-2575-9684; Email: mahmou22@msu.edu

Mohammad Raoufi − *Nanotechnology Research Center, Faculty of Pharmacy, Tehran University of Medical Sciences, Tehran 13169-43551, Iran; Physical Chemistry I, Department of Chemistry and Biology & Research Center of Micro and Nanochemistry and Engineering (Cμ), University of Siegen, Siegen 57076, Germany*; Email: raoufi@chemie.uni-siegen.de

Authors

Rahimeh B. Atashgah − *Colloids and Polymers Physics Group, Particle Physics Department, Faculty of Physics and Health Research Institute of Santiago de Compostela (IDIS), Universidade de Santiago de Compostela, 15782 Santiago de Compostela, Spain; Department of Pharmaceutical Biomaterials and Medical Biomaterials Research Center, Faculty of Pharmacy, Tehran University of Medical Sciences, Tehran 14167-53955, Iran*

Amir Ghasemi − *Nanotechnology Research Center, Faculty of Pharmacy, Tehran University of Medical Sciences, Tehran 13169-43551, Iran*

Mohammad-Amin Abdollahifar − *Department of Biology and Anatomical Sciences, School of Medicine, Shahid Beheshti University of Medical Sciences, Tehran 19395-4719, Iran*

Steven Zanganeh − *Department of Bioengineering, University of Massachusetts Dartmouth, Dartmouth, Massachusetts 02747, United States*

Hossein Nejadnik − *Department of Radiology, University of Pennsylvania, Philladelphia, Pennsylvania 19104, United States*

Alieh Abdollahi − *Department of Pharmaceutical Biomaterials and Medical Biomaterials Research Center, Faculty of Pharmacy, Tehran University of Medical Sciences, Tehran 14167-53955, Iran*

Shahriar Sharifi − *Precision Health Program, Michigan State University, East Lansing, Michigan 48824, United States;* orcid.org/0000-0002-3853-5428

Baltazar Lea − *Colloids and Polymers Physics Group, Particle Physics Department, Faculty of Physics and Health Research Institute of Santiago de Compostela (IDIS), Universidade de Santiago de Compostela, 15782 Santiago de Compostela, Spain*

Miguel Cuerva − *NANOMAG Group, Technological Research Institute (IIT), Physical Chemistry Department, University of Santiago de Compostela (USC), Santiago de Compostela 15782, Spain*

Mehdi Akbarzadeh − *Sadra Wound, Ostomy and Osteomyelitis Specialist Center, Tehran, Iran*

Carmen Alvarez-Lorenzo − *R+D Pharma Group, Pharmacology, Pharmacy and Pharmaceutical Technology Department, Faculty of Pharmacy and Health Research Institute of Santiago de Compostela (IDIS), Universidade de Santiago de Compostela, 15782 Santiago de Compostela, Spain;* orcid.org/0000-0002-8546-7085

Seyed Nasser Ostad − *Department of Pharmaceutical Biomaterials and Medical Biomaterials Research Center, Faculty of Pharmacy, Tehran University of Medical Sciences, Tehran 14167-53955, Iran*

Andrea S. Theus − *Wallace H. Coulter Department of Biomedical Engineering, Emory University School of Medicine and Georgia Institute of Technology, Atlanta, Georgia 30322, United States;* orcid.org/0000-0001-5399-2910

Doris L. LaRock − *Department of Microbiology and Immunology, Emory Antibiotic Resistance Center, Emory University School of Medicine, Atlanta, Georgia 30322, United States*

Christopher N. LaRock − *Department of Microbiology and Immunology, Emory Antibiotic Resistance Center, Emory University School of Medicine, Atlanta, Georgia 30322, United States;* orcid.org/0000-0003-3035-5331

Vahid Serpooshan − *Wallace H. Coulter Department of Biomedical Engineering, Emory University School of Medicine and Georgia Institute of Technology, Atlanta, Georgia 30322, United States; Department of Pediatrics, Emory University School of Medicine, Atlanta, Georgia 30309, United States; Children's Healthcare of Atlanta, Atlanta, Georgia 30322, United States;* orcid.org/0000-0002-5304-095X

Rouzbeh Sarrafi − *SciDerm, Natick, Massachusetts, United States*

Ki-Bum Lee − *Department of Chemistry and Chemical Biology, Rutgers, The State University of New Jersey, Piscataway, New Jersey 08854, United States*

Hojatollah Vali − *Department of Anatomy and Cell Biology and Facility for Electron Microscopy Research, McGill University, Montreal, Quebec H3A 0C3, Canada*

Holger Schönherr − *Physical Chemistry I, Department of Chemistry and Biology & Research Center of Micro and Nanochemistry and Engineering (Cμ), University of Siegen, Siegen 57076, Germany;* orcid.org/0000-0002-5836-5569

Lisa Gould − *Brown University School of Medicine, Providence, Rhode Island 02903, United States; South Shore*

https://doi.org/10.1021/acs.molpharmaceut.1c00400
Mol. Pharmaceutics 2021, 18, 3171−3180

Health System Center for Wound Healing, Weymouth, Massachusetts 02189, United States

Pablo Taboada − *Colloids and Polymers Physics Group, Particle Physics Department, Faculty of Physics and Health Research Institute of Santiago de Compostela (IDIS), Universidade de Santiago de Compostela, 15782 Santiago de Compostela, Spain;* orcid.org/0000-0002-2903-7857

Complete contact information is available at: https://pubs.acs.org/10.1021/acs.molpharmaceut.1c00400

Notes

The authors declare the following competing financial interest(s): Dr. Mahmoudi discloses that (i) he is a co-founder and director of the Academic Parity Movement, a non-profit organization dedicated to addressing academic discrimination, violence and incivility; (ii) he is a Founding Partner at Partners in Global Wound Care (PGWC); and (iii) he receives royalties/honoraria for his published books, plenary lectures, and licensed patent. Dr. Raoufi is a Founding Partner at PGWC.

■ ACKNOWLEDGMENTS

This work was supported by the following grants: 2018 BRIght Future Prize from BWH, FEDER, and NSF (award no. 1945779). P.T. thanks MINECO for funding through grant MAT2016-80266-R, and Xunta de Galicia for additional financial support (Agrupación Estratégica de Materiales, Action ED431E 2018/08, and Grupos de Referencia Competitiva, Action ED431C 2018/26).

■ REFERENCES

(1) Nunan, R.; Harding, K. G.; Martin, P. Clinical challenges of chronic wounds: searching for an optimal animal model to recapitulate their complexity. *Dis. Models & Mech.* **2014**, *7*, 1205−1213.

(2) Bryant, R.; Nix, D. *Acute and Chronic Wounds-E-Book*; Elsevier Health Sciences, 2015.

(3) Stone, R. C.; et al. A bioengineered living cell construct activates an acute wound healing response in venous leg ulcers. *Sci. Transl. Med.* **2017**, *9*, eaaf8611.

(4) Eming, S. A.; Martin, P.; Tomic-Canic, M. Wound repair and regeneration: mechanisms, signaling, and translation. *Sci. Transl. Med.* **2014**, *6*, 265sr6.

(5) *I-Corps: Multifunctional Patch for Chronic Wounds*; National Science Foundation, 2019; award no. 1945779https://www.nsf.gov/awardsearch/showAward?AWD_ID=1945779 (accessed on 2021-07-07).

(6) Boateng, J. S.; Matthews, K. H.; Stevens, H. N.; Eccleston, G. M. Wound healing dressings and drug delivery systems: a review. *J. Pharm. Sci.* **2008**, *97*, 2892−2923.

(7) Ovington, L. G. Advances in wound dressings. *Clinics in dermatology* **2007**, *25*, 33−38.

(8) Falanga, V.; Sabolinski, M. A bilayered living skin construct (APLIGRAF®) accelerates complete closure of hard-to-heal venous ulcers. *Wound Repair and Regeneration* **1999**, *7*, 201−207.

(9) Ikada, Y. Challenges in tissue engineering. *J. R. Soc., Interface* **2006**, *3*, 589−601.

(10) Gurtner, G. C.; Werner, S.; Barrandon, Y.; Longaker, M. T. Wound repair and regeneration. *Nature* **2008**, *453*, 314.

(11) Bello, Y. M.; Falabella, A. F.; Eaglstein, W. H. Tissue-engineered skin. *American journal of clinical dermatology* **2001**, *2*, 305−313.

(12) Zhong, S.; Zhang, Y.; Lim, C. Tissue scaffolds for skin wound healing and dermal reconstruction. *Wiley Interdiscip. Rev.: Nanomed. Nanobiotechnol.* **2010**, *2*, 510−525.

(13) Dreifke, M. B.; Jayasuriya, A. A.; Jayasuriya, A. C. Current wound healing procedures and potential care. *Mater. Sci. Eng., C* **2015**, *48*, 651−662.

(14) Jayakumar, R.; Prabaharan, M.; Sudheesh Kumar, P. T.; Nair, S.; Tamura, H. Biomaterials based on chitin and chitosan in wound dressing applications. *Biotechnol. Adv.* **2011**, *29*, 322−337.

(15) Snyder, D. L.; Sullivan, N.; Schoelles, K. M. *Skin Substitutes for Treating Chronic Wounds*; Agency for Healthcare Research and Quality: Rockville, MD, 2012).

(16) Zhou, B.; Lu, Y.; Hajifathalian, K.; Bentham, J.; Di Cesare, M.; Danaei, G.; Bixby, H.; Cowan, M. J.; Ali, M. K.; Taddei, C.; et al. Worldwide Trends in Diabetes since 1980: a Pooled Analysis of 751 Population-Based Studies with 4.4 Million Participants. *Lancet* **2016**, *387*, 1513−1530.

(17) Balasubramani, M.; Kumar, T. R.; Babu, M. Skin substitutes: a review. *Burns* **2001**, *27*, 534−544.

(18) Dickinson, L. E.; Gerecht, S. Engineered Biopolymeric Scaffolds for Chronic Wound Healing. *Front. Physiol.* **2016**, *7*, 341.

(19) Sharifi, S.; Hajipour, M. J.; Gould, L.; Mahmoudi, M. Nanomedicine in Healing Chronic Wounds: Opportunities and Challenges. *Mol. Pharmaceutics* **2021**, *18*, 550−575.

(20) Falanga, V. Wound healing and its impairment in the diabetic foot. *Lancet* **2005**, *366*, 1736−1743.

(21) James, G. A.; Swogger, E.; Wolcott, R.; deLancey Pulcini, E.; Secor, P.; Sestrich, J.; Costerton, J. W.; Stewart, P. S. Biofilms in chronic wounds. *Wound Repair Regen.* **2008**, *16*, 37−44.

(22) Dvir, T.; Timko, B. P.; Kohane, D. S.; Langer, R. Nanotechnological strategies for engineering complex tissues. *Nat. Nanotechnol.* **2011**, *6*, 13−22.

(23) Zhong, S. P.; Zhang, Y. Z.; Lim, C. T. Tissue scaffolds for skin wound healing and dermal reconstruction. *Nanomed. Nanobiotechnol.* **2010**, *2*, 510−525.

(24) Goy, R. C.; Morais, S. T.; Assis, O. B. Evaluation of the antimicrobial activity of chitosan and its quaternized derivative on E. coli and S. aureus growth. *Rev. Bras. Farmacogn.* **2016**, *26*, 122−127.

(25) Mahmoudi, M.; Serpooshan, V. Silver-coated engineered magnetic nanoparticles are promising for the success in the fight against antibacterial resistance threat. *ACS Nano* **2012**, *6*, 2656−2664.

(26) Subbiahdoss, G.; et al. Magnetic targeting of surface-modified superparamagnetic iron oxide nanoparticles yields antibacterial efficacy against biofilms of gentamicin-resistant staphylococci. *Acta Biomater.* **2012**, *8*, 2047−2055.

(27) Zanganeh, S.; et al. Iron oxide nanoparticles inhibit tumour growth by inducing pro-inflammatory macrophage polarization in tumour tissues. *Nat. Nanotechnol.* **2016**, *11*, 986.

(28) Zanganeh, S.; et al. Tumor-associated macrophages, nano-medicine and imaging: the axis of success in the future of cancer immunotherapy. *Immunotherapy* **2017**, *9*, 819−835.

(29) Khanna, S.; et al. Macrophage dysfunction impairs resolution of inflammation in the wounds of diabetic mice. *PLoS One* **2010**, *5*, e9539.

(30) Hesketh, M.; Sahin, K. B.; West, Z. E.; Murray, R. Z. Macrophage phenotypes regulate scar formation and chronic wound healing. *Int. J. Mol. Sci.* **2017**, *18*, 1545.

(31) Krzyszczyk, P.; Schloss, R.; Palmer, A.; Berthiaume, F. The role of macrophages in acute and chronic wound healing and interventions to promote pro-wound healing phenotypes. *Front. Physiol.* **2018**, *9*, 3389.

(32) Wei, K.; et al. Epicardial FSTL1 reconstitution regenerates the adult mammalian heart. *Nature* **2015**, *525*, 479.

(33) Mattiotti, A.; Prakash, S.; Barnett, P.; van den Hoff, M. J. Follistatin-like 1 in development and human diseases. *Cell. Mol. Life Sci.* **2018**, *75*, 2339−2354.

(34) Sundaram, G. M.; et al. 'See-saw' expression of microRNA-198 and FSTL1 from a single transcript in wound healing. *Nature* **2013**, *495*, 103.

(35) Herter, E. K.; Landen, N. X. Non-Coding RNAs: New Players in Skin Wound Healing. *Adv. Wound Care* **2017**, *6*, 93−107.

(36) Strauss, J. F.; Barbieri, R. L. *Yen & Jaffe's Reproductive Endocrinology E-Book: Physiology, Pathophysiology, and Clinical Management*; Elsevier Health Sciences, 2013.
(37) Harrison, C. A.; Gray, P. C.; Vale, W. W.; Robertson, D. M. Antagonists of activin signaling: mechanisms and potential biological applications. *Trends Endocrinol. Metab.* **2005**, *16*, 73−78.
(38) Antsiferova, M.; Werner, S. The bright and the dark sides of activin in wound healing and cancer. *J. Cell Sci.* **2012**, *125*, 3929.
(39) Mukhopadhyay, A.; Chan, S. Y.; Lim, I. J.; Phillips, D. J.; Phan, T. T. The role of the activin system in keloid pathogenesis. *American Journal of Physiology-Cell Physiology* **2007**, *292*, C1331−C1338.
(40) Mahmoudi, M.; et al. Multiscale technologies for treatment of ischemic cardiomyopathy. *Nat. Nanotechnol.* **2017**, *12*, 845.
(41) Perretti, M.; et al. Endogenous lipid-and peptide-derived anti-inflammatory pathways generated with glucocorticoid and aspirin treatment activate the lipoxin A 4 receptor. *Nat. Med.* **2002**, *8*, 1296.
(42) Krishnamoorthy, S.; et al. Resolvin D1 binds human phagocytes with evidence for proresolving receptors. *Proc. Natl. Acad. Sci. U. S. A.* **2010**, *107*, 1660−1665.
(43) Fredman, G.; Kamaly, N.; Spolitu, S.; Milton, J.; Ghorpade, D.; Chiasson, R.; Kuriakose, G.; Perretti, M.; Farokhzad, O.; Tabas, I. Targeted nanoparticles containing the proresolving peptide Ac2−26 protect against advanced atherosclerosis in hypercholesterolemic mice. *Sci. Transl. Med.* **2015**, *7*, 275ra20.
(44) Kamaly, N.; et al. Development and in vivo efficacy of targeted polymeric inflammation-resolving nanoparticles. *Proc. Natl. Acad. Sci. U. S. A.* **2013**, *110*, 6506−6511.
(45) Leoni, G.; et al. Annexin A1−containing extracellular vesicles and polymeric nanoparticles promote epithelial wound repair. *J. Clin. Invest.* **2015**, *125*, 1215−1227.
(46) Del Gaudio, P.; et al. Evaluation of in situ injectable hydrogels as controlled release device for ANXA1 derived peptide in wound healing. *Carbohydr. Polym.* **2015**, *115*, 629−635.
(47) Chen, Y.-M.; Chung, Y.-C.; Woan Wang, L.; Chen, K.-T.; Li, S.-Y. Antibacterial properties of chitosan in waterborne pathogen. *J. Environ. Sci. Health, Part A: Toxic/Hazard. Subst. Environ. Eng.* **2002**, *37*, 1379−1390.
(48) Sarasam, A. R.; Krishnaswamy, R. K.; Madihally, S. V. Blending chitosan with polycaprolactone: effects on physicochemical and antibacterial properties. *Biomacromolecules* **2006**, *7*, 1131−1138.
(49) Mahdy Samar, M.; El-Kalyoubi, M.H.; Khalaf, M.M.; Abd El-Razik, M.M. Physicochemical, functional, antioxidant and antibacterial properties of chitosan extracted from shrimp wastes by microwave technique. *Ann. Agric. Sci.* **2013**, *58*, 33−41.
(50) Vaz, J. M.; et al. Antibacterial properties of chitosan-based coatings are affected by spacer-length and molecular weight. *Appl. Surf. Sci.* **2018**, *445*, 478−487.
(51) Yang, K.; et al. Effect of syringic acid incorporation on the physical, mechanical, structural and antibacterial properties of chitosan film for quail eggs preservation. *Int. J. Biol. Macromol.* **2019**, *141*, 876−884.
(52) Twardowski, T.; Fertala, A.; Orgel, J.; San Antonio, J. Type I collagen and collagen mimetics as angiogenesis promoting superpolymers. *Curr. Pharm. Des.* **2007**, *13*, 3608−3621.
(53) Feng, X.; Tonnesen, M. G.; Mousa, S. A.; Clark, R. A. Fibrin and collagen differentially but synergistically regulate sprout angiogenesis of human dermal microvascular endothelial cells in 3-dimensional matrix. *Int. J. Cell Biol.* **2013**, *2013*, 231279.
(54) van Kempen, L. C.; et al. Type I collagen expression contributes to angiogenesis and the development of deeply invasive cutaneous melanoma. *Int. J. Cancer* **2008**, *122*, 1019−1029.
(55) Nicosia, R. F.; Belser, P.; Bonanno, E.; Diven, J. Regulation of angiogenesis in vitro by collagen metabolism. *In Vitro Cell. Dev. Biol.* **1991**, *27*, 961−966.
(56) Altman, R.; et al. Anti-inflammatory effects of intra-articular hyaluronic acid: a systematic review. *Cartilage* **2019**, *10*, 43−52.
(57) Gocmen, G.; Gonul, O.; Oktay, N. S.; Yarat, A.; Goker, K. The antioxidant and anti-inflammatory efficiency of hyaluronic acid after third molar extraction. *Journal of Cranio-Maxillofacial Surgery* **2015**, *43*, 1033−1037.
(58) Chang, C. H.; et al. Anti-inflammatory effects of hydrophilic and lipophilic statins with hyaluronic acid against LPS-induced inflammation in porcine articular chondrocytes. *J. Orthop. Res.* **2014**, *32*, 557−565.
(59) Sheibani, S.; Basu, K.; Farnudi, A.; Ashkarran, A.; Ichikawa, M.; Presley, J. F.; Bui, K. H.; Ejtehadi, M. R.; Vali, H.; Mahmoudi, M. Nanoscale characterization of the biomolecular corona by cryo-electron microscopy, cryo-electron tomography, and image simulation. *Nat. Commun.* **2021**, *12*, 573.
(60) Dawson, K. A.; Yan, Y. Current understanding of biological identity at the nanoscale and future prospects. *Nat. Nanotechnol.* **2021**, *16*, 229−242.
(61) Ke, P. C.; Lin, S.; Parak, W. J.; Davis, T. P.; Caruso, F. A decade of the protein corona. *ACS Nano* **2017**, *12*, 11773−11776.
(62) Salvador-Morales, C.; Zhang, L.; Langer, R.; Farokhzad, O. C. Immunocompatibility properties of lipid−polymer hybrid nanoparticles with heterogeneous surface functional groups. *Biomaterials* **2009**, *30*, 2231−2240.
(63) Monopoli, M. P.; Åberg, C.; Salvati, A.; Dawson, K. A. Biomolecular coronas provide the biological identity of nanosized materials. *Nat. Nanotechnol.* **2012**, *7*, 779.
(64) Frank, S.; et al. Regulation of vascular endothelial growth factor expression in cultured keratinocytes. Implications for normal and impaired wound healing. *J. Biol. Chem.* **1995**, *270*, 12607−12613.
(65) Barrientos, S.; Stojadinovic, O.; Golinko, M. S.; Brem, H.; Tomic-Canic, M. Growth factors and cytokines in wound healing. *Wound repair and regeneration* **2008**, *16*, 585−601.
(66) Unemori, E.; Hibbs, M.; Amento, E. Constitutive expression of a 92-kD gelatinase (type V collagenase) by rheumatoid synovial fibroblasts and its induction in normal human fibroblasts by inflammatory cytokines. *J. Clin. Invest.* **1991**, *88*, 1656−1662.
(67) So, T.; Ito, A.; Sato, T.; Mori, Y.; Hirakawa, S. Tumor Necrosis Factor-α Stimulates the Biosynthesis of Matrix Metafloproteinases and Plasminogen Activator in Cultured Human Chorionic Cells. *Biol. Reprod.* **1992**, *46*, 772−778.
(68) Rawdanowicz, T.; Hampton, A.; Nagase, H.; Woolley, D.; Salamonsen, L. Matrix metalloproteinase production by cultured human endometrial stromal cells: identification of interstitial collagenase, gelatinase-A, gelatinase-B, and stromelysin-1 and their differential regulation by interleukin-1 alpha and tumor necrosis factor-alpha. *J. Clin. Endocrinol. Metab.* **1994**, *79*, 530−536.
(69) Ågren, M. S.; Taplin, C. J.; Woessner, J. F., Jr; Eagistein, W. H.; Mertz, P. M. Collagenase in wound healing: effect of wound age and type. *J. Invest. Dermatol.* **1992**, *99*, 709−714.
(70) Gill, S. E.; Parks, W. C. Metalloproteinases and their inhibitors: regulators of wound healing. *Int. J. Biochem. Cell Biol.* **2008**, *40*, 1334−1347.
(71) Armstrong, D. G.; Jude, E. B. The role of matrix metalloproteinases in wound healing. *Journal of the American Podiatric Medical Association* **2002**, *92*, 12−18.
(72) Hajipour, M. J.; Aghaverdi, H.; Serpooshan, V.; Vali, H.; Sheibani, S.; Mahmoudi, M. Sex as an important factor in nanomedicine. *Nat. Commun.* **2021**, *12*, 2964.
(73) Sharifi, S.; Caracciolo, G.; Pozzi, D.; Digiacomo, L.; Swann, J.; Daldrup-Link, H. E.; Mahmoudi, M. The role of sex as a biological variable in the efficacy and toxicity of therapeutic nanomedicine. *Adv. Drug Delivery Rev.* **2021**, *174*, 337.
(74) Vanić, Ž.; Wenche Jøraholmen, M. W.; Škalko-Basnet, N. Nanomedicines for the topical treatment of vulvovaginal infections: addressing the challenges of antimicrobial resistance. *Adv. Drug Delivery Rev.* **2021**, 113855.

https://doi.org/10.1021/acs.molpharmaceut.1c00400
Mol. Pharmaceutics 2021, 18, 3171−3180